The University of South Bohemia in České Budějovice
Faculty of Science

An analysis of fungal exudate and carbon use efficiency

Bachelor thesis

Laura Nübl

Advisor: RNDr. Travis B. Meador, Ph.D.

České Budějovice 2022

Nübl L. 2022: An analysis of fungal exudate and carbon use efficiency. Bc. Thesis, in English – 29 p. Faculty of Science, University of South Bohemia, České Budějovice, Czech Republic.

Annotation:
The exometabolome of various fungal functional guilds was investigated as part of the below-ground carbon flux. This thesis addresses the incorporation and exudation of carbon by individual, axenic fungal cultures, with a focus on developing a protocol for characterisation and identification of those compounds.

Declaration:
I declare that I am the author of this qualification thesis and that in writing it I have used the sources and literature displayed in the list of used sources only.

Linz, 26.02.2022 .....
Laura Nübl

Table of Contents

Introduction....1
1.1 The Carbon Cycle....1
1.2 The Role of Fungi in the Below Ground Carbon Flux....1
1.3 Fungal Diversity....2
1.4 Metabolic Diversity and Metabolomics....2
1.5 Mass Spectrometry-based, Untargeted Metabolomics....3
1.6 Isotopic Labelling in Metabolomics....3
1.6.1 Stable Isotope Notations....3
2 Aims....4
3 Materials and Methods....5
3.1 Chemicals....5
3.2 Culturing....5
3.2.1 Production of Fungal Inocula....5
3.2.2 Preparation of Base Medium....6
3.2.3 Preparation of Cultures....7
3.2.4 Fungal Growth....7
3.2.4.1 Growth....8
3.2.4.2 Carbon Use Efficiency....8
3.2.5 Harvesting....9
3.3 Sample Processing....9
3.3.1 Filtration....9
3.3.2 Extraction....9
3.4 UV-visible Spectroscopy Analyses....9
3.4.1 ABTS Antioxidant Assay....9
3.4.2 Total Medium Extract Absorbance....11
3.5 Isotope Ratio Mass Spectrometry....12
3.5.1 Preparation for Elemental Analysis....12
3.5.2 Compound Specific Isotope Analysis....12
3.6 Derivatization of TME for GC analyses....12
3.6.1 Acetylation....12
3.6.2 Trimethylsilylation....12
3.7 Gas Chromatography-Mass Spectrometry Analysis....13
3.8 Gas Chromatography-Mass Spectrometry Data Analysis....13
3.8.1 Acetylated TME....13
3.8.2 Trimethylsilylated TME....14
4 Results....15
4.1 Culturing....15
4.1.1 Growth....15
4.1.2 Carbon Use Efficiency....16
4.2 Antioxidant Assay....17
4.3 Total Medium Extract Absorbance....18
4.4 Isotope Ratio Mass Spectrometry....19
4.5 Gas Chromatography-Mass Spectrometry analysis....19
4.5.1 Acetylated TME....19
4.5.2 Trimethylsilylated TME....22
5 Discussion....24
5.1 Culturing....24
5.1.1 Growth....24

5.1.2 Carbon Use Efficiency....24
5.2 Antioxidant Assay....24
5.3 Total Medium Extract Absorbance....25
5.4 Isotope Ratio Mass Spectrometry....25
5.4.1 Elemental Analysis....25
5.4.2 Compound Specific Isotope Analysis....25
5.5 Derivatization....25
5.5.1 Acetylation....25
5.5.2 Trimethylsilylation....26
5.6 Gas Chromatography-Mass Spectrometry Data Analysis....26
5.6.1 Acetylation....26
5.6.2 Trimethylsilylation....26
5.7 Future work....28
6 Conclusion....29
7 References....30
8 Appendix....33
8.1 List of possible quinone fragments....33

List of Abbreviations

SOM	Soil Organic Matter
EMF	Ectomycorrhizal Fungi
MS	Mass Spectrometry
GC-MS	Gas Chromatography-Mass Spectrometry
LC-MS	Liquid Chromatography-Mass Spectrometry
IRMS	Isotope Ratio Mass Spectrometry
CYA	Czapec Yeast Agar
MQ	MilliQ
AB	*Aspergillus brasiliensis*
CF	*Cordyceps farinosa*
YL	*Yarrowia lipolytica*
PC	*Phanerodontia chrysosporium*
AP	*Acremonium polychromum*
PJ	*Penicillium janczewskii*
AD	*Aspergillus dimorphicus*
PVDF	Polyvinylidene Fluoride
TDC	Thermal Conductivity Detector
CUE	Carbon Use Efficiency
GF	Glass Filter
TME	Total Medium Extract
UV	Ultra Violet
UV-Vis	Ultra Violet-Visible
TEAC	Trolox Equivalent Antioxidant Capacity

ACN	Acetonitrile
CSIA	Compound Specific Isotope Analysis
EA-IRMS	Elemental Analysis-IRMS
TMS	Trimethylsilyl/ation
FID	Flame Ionisation Detector
TIC	Total Ion Current
NIST	National Institute of Standards and Technology
DMMK	Dimethylmenaquinone
UQ	Ubiquinone
MCD	Multi-Channel Device
EI	Electron Impact Ionisation

Introduction

1.1 The Carbon Cycle

Carbon is one of the most abundant, as well as stable elements on earth. It forms the basis of all living organisms – making up about 50% of their dry weight. Its movement, in its various forms, through the major reservoirs, approximates the flow of energy around the earth[1] and is known as the global carbon cycle. Of the five major global carbon pools (Fig. 1): oceanic, geologic, pedologic, atmospheric, and biotic, the terrestrial reservoir is made up of the biotic and pedologic pools and is the third largest carbon storage on earth[2]. The flux of carbon from the atmospheric to the terrestrial reservoir is, primarily, photosynthesis[3]. Once in the soil, however, there are numerous fluxes and pathways for this freshly sequestered carbon, many of which are difficult to observe or unknown entirely.[4]

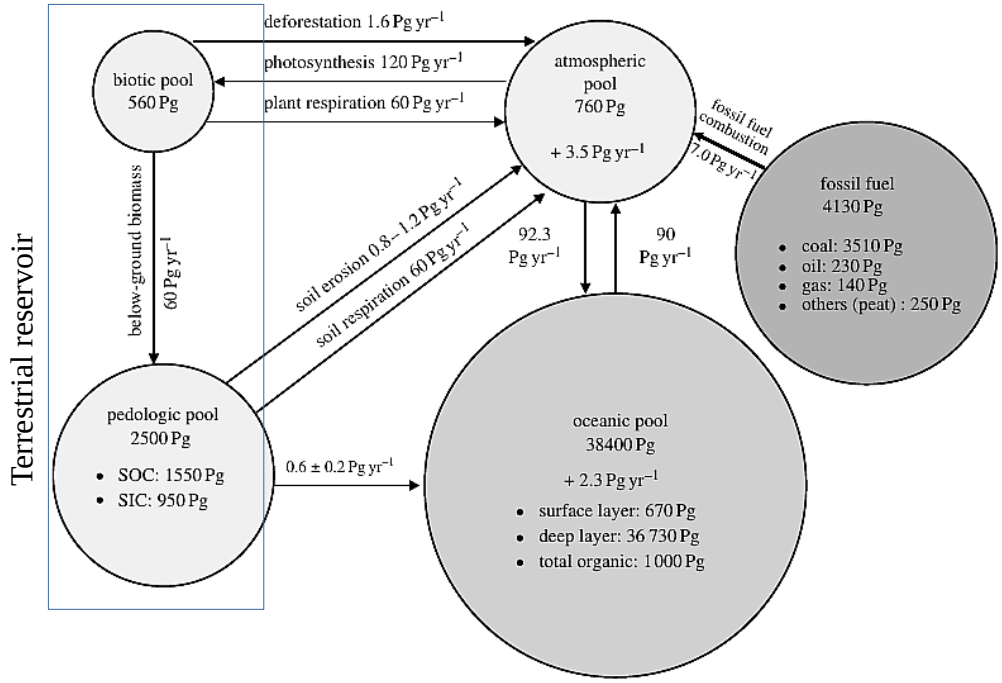

Figure 1: Main pools in the global carbon cycle and fluxes between them as published by R. Lal[2]; the blue rectangle indicates the terrestrial carbon reservoir

1.2 The Role of Fungi in the Below Ground Carbon Flux

Fungi are among the most diverse and widespread organisms on earth. Its members are ubiquitous in nature and play a part in all major ecosystems[5]. Filamentous fungi have succeeded in colonising most natural environments via their expansive mycelial networks[6], which are known to span from microscopic to many square metres[7]. Furthermore, the

filaments making up this network can be activated and inactivated as needed by moving cytoplasm into and out of the tubular hyphae[8]. These characteristics allow for fungi to closely associate with plant fine roots, where they then have privileged access to carbohydrates and other labile root exudates[9].

Being heterotrophs, fungi are reliant on reduced C, which mycorrhizal fungi largely receive from their host plants[3]; Some of them, however, can mineralise soil organic matter (SOM) directly – though often rather for the mineral nutrients captured in it and ignoring the C fraction[3]. Therefore, according to Lindhal and Tunlid (2015), "*Under the assumption that ectomycorrhizal fungi (EMF) approach organic matter primarily as a source of N than metabolic C, it may not be a given that C is decomposed all the way to CO_2 and lost from the system*"[10]. Saprotrophic fungi, on the other hand, have the ability to break down phenolic compounds in SOM using various extracellular oxidative enzymes and secondary metabolites[11]. These fungal mechanisms greatly affect a number of soil processes including the composition and activity of microbial communities[3].

1.3 Fungal Diversity

The diversity of fungi in the soil is vast, with one study finding more than 800 species in 1g of soil[12]. While the traditional phylogenetic classification is based on genetic relatedness, this system does not account for widely differing methods of resource exploitation, or 'functional guilds' that are polyphyletic across Ascomycota and Basidiomycota[13]. Furthermore, according to multiple microcosm and laboratory studies, there is additional niche partitioning in these soil fungi with species "*varying widely in their traits of ecological interest, such as the range of polymers their enzymes are adapted to attack, edaphic preferences, hyphal foraging strategies, host specificity, and dispersal and root colonisation strategies*"[12].

1.4 Metabolic Diversity and Metabolomics

The various strategies of resource capture displayed by soil fungi also require specialised metabolisms. This field of research, called metabolomics, has been extensively studied – with over 30 000 secondary metabolites identified as fungal products – not only for taxonomic purposes via chemical fingerprinting, but also for the many bioactive compounds produced by fungi[14].

In the below ground carbon flux, however, a very important factor is not what is produced internally, but what is excreted by fungi. This component of fungal metabolic activity, that is

intended for interaction with the environment, is called the exometabolome[14], and is made up of compounds produced by the mycelium that can affect and potentially be consumed by other soil organisms[3].

1.5 Mass Spectrometry-based, Untargeted Metabolomics

Technical, as well as methodological developments, have considerably advanced the field of metabolomics in recent years[15]. Most often, a Chromatography-Mass Spectrometry (MS) based approach is used due to its speed and sensitivity[16], and the fact that, when using a non-targeted approach, known sample composition is not needed to detect metabolites[15]. This is especially true when using a hard ionisation technique like Electron Impact Ionisation (EI) as the resulting ionic fragments and fragment patterns allow for more accurate assignment. However, identification, and assignment of structures to spectra in untargeted analysis is strongly dependent on the spectral resolution, as well as the availability of standards, reported spectra in literature, or spectral databases. Accurate identification is therefore labour intensive, and unambiguous assignment not always achievable[15]. Nevertheless, MS is the current gold standard in the field of metabolomics[17], especially since a full structure elucidation is not always necessary.

1.6 Isotopic Labelling in Metabolomics

Stable isotopic labelling, via the addition of one or more stable isotopes (like ^{13}C or ^{2}H), can be used to trace the utilisation and biosynthesis of specific compounds by natural organisms or systems. Even within complex mixtures of metabolites, these stable isotopes are easily distinguishable from more common natural isotopes (like ^{12}C and ^{1}H) via highly sensitive Isotope Ratio Mass Spectrometry (IRMS). The measurement of these isotopic ratios therefore allows for identification and tracking of biologically synthesised compounds[18], and is often used in combination with gas chromatography as a separation technique.

1.6.1 Stable Isotope Notations

At natural abundance levels, the isotopic differences of materials are minute, so ratios are reported in parts per thousand (per mil) relative to an internationally recognised standard[19]. For carbon, the two stable isotopes are ^{12}C, with an abundance of 98.89%, and the less common ^{13}C, with an abundance of 1.11%[19]. The $\delta^{13}C$ is then calculated as:

$$\delta 13C(‰) = \left(\left[\frac{C^{13}}{C^{12}}_{sample}\right] - 1\right) \times 1000$$

$$\left[\frac{C^{13}}{C^{12}}\right]_{standard}$$

2 Aims

- Grow axenic cultures of a variety of fungal species and harvest compounds exuded into media culture
- Calculate Carbon Use Efficiency of individual fungal species
- Determine antioxidant activity of compounds exuded into medium
- Estimate fraction of water-derived hydrogen (H) and inorganic carbon (C) substrates incorporated into exudates
- Develop GC-MS protocols to identify exuded compounds in fungal growth medium and determine their stable C and H isotopic composition

3 Materials and Methods

3.1 Chemicals

Potassium peroxodisulphate (>=99%), ABTS diammonium salt (>=98%), trolox (97%), pyridine anhydrous (99.8%), BSTFA (for GC derivatisation; 99%), 1-methyl imidazole (99% reagent plus), acetic anhydride (99% reagent plus) were purchased from Sigma-Aldrich (Czech Republic); Sodium acetate trihydrate (>=99%) by Penta chemicals unlimited (Czech Republic); *n*-Hexane (for trace analysis), dichloromethane (for trace analysis), and ethyl acetate (for trace analysis) by VWR (Belgium); Methanol (LC-MS grade) by J.T. Baker (Netherlands); Acetic acid (99.8%) by Lachner (Czech Republic); Acetonitrile (HPLC grade) by Honeywell (France)

3.2 Culturing

3.2.1 Production of Fungal Inocula

Cultures of different fungal species with a variety of ecotypes were obtained from the Biology Centre Collection of Organisms – Institute of Soil Biology, with the exception of: *Yarrowia lipolytica*, which was part of the Belgian Co-ordinated Collections of Microorganisms / Mycothèque de l'Université Catholique de Louvain; *Aspergillus brasiliensis*, which was a part of the Culture Collection of Fungi at the Charles University, Prague; and *Phanerodontia chrysosporium,* from the Czech Collection of Microorganisms (CCM), Masaryk University, Faculty of Science, Brno. Conidia of the fungi were cultured under non-stressed conditions to inoculate into the liquid medium. The inocula were grown on 95mm Polystyrene Petri dishes on Czapec Yeast Agar (CYA), and were incubated in the dark at 25°C. The harvested conidia were then suspended in 40mL of MiliQ sterile water (MQ) to produce a concentration of approximately 10^6 conidia mL^{-1}. This suspension was shaken and filtered through sterile double cheesecloth, before being washed twice via centrifugation in MQ at 7000xg for 3 minutes at 25℃.

Table 1: Fungal species included in exudate study

#	Fungal species	Strain number	Culture Collection
1	*Aspergillus dimorphicus* B.S. Mehrotra & R. Prasad	BCCO 20_2442	Biology Centre Collection of Organisms – Institute of Soil Biology
2	*Aspergillus brasiliensis* (former *Aspergillus niger)*	CCM 8222	Culture Collection of Fungi – Charles University Prague
3	*Penicillium janczewskii* K.W. Zaleski	BCCO 20_0265	Biology Centre Collection of Organisms – Institute of Soil Biology
4	*Acremonium polychromum* (J.F.H. Beyma) W. Gams	BCCO 20_1588	Biology Centre Collection of Organisms – Institute of Soil Biology
5	*Cordyceps farinosa* (Holmsk.) Kepler, B. Shrestha & Spatafora (accepted name) - *Isaria farinosa* (Holmsk.) Fr. (synonym)	BCCO 20_1579	Biology Centre Collection of Organisms – Institute of Soil Biology
6*	*Yarrowia lipolytica (Wickerham, Kurtzman & Herman) van der Walt & von Arx*	MUCL 054012	Belgian Co-ordinated Collections of Microorganisms / Mycothèque de l'Université Catholique de Louvain
7*	*Phanerodontia chrysosporium* (Burds.) Hjortstam & Ryvarden (accepted name) - *Phanerochaete chrysosporium* Burds. (synonym)	CCM 8074^{T}	Czech Collection of Microorganisms (CCM), Masaryk University, Faculty of Science, Brno

** species 6 and 7 did not achieve satisfactory growth and were therefore excluded from further analyses*

3.2.2 Preparation of Base Medium

A modified version of the Czapek[20]-Dox[21] Broth, approximate recipe per litre below, was prepared according to Thom and Raper[22], with the carbon source changed to D-(+)-glucose, and the carbon content lowered to 4 gC L^{-1}, or 10g of glucose per litre.

Table 2: Adjusted Czapec-Dox broth recipe; components per litre At 25°C pH 7.3 ± 0.2

Glucose	10.0 g
Sodium nitrate	3.0 g
Dipotassium phosphate	1.0 g
Magnesium sulphate	0.5 g
Potassium chloride	0.5 g
Ferrous sulphate	0.01 g

Inorganic carbon in the form of sodium bicarbonate ($NaHCO_3$) was added at 0.9g L^{-1}, while isotopic labelling was applied via ^{13}C-labelled $NaHCO_3$ at 9mg L^{-1-}, and three different doses of D_2O (δ^2H at 100‰, 200‰, and 400‰). These solutions were then sterile filtered (Millex® GV filter unit 0.22 µm pore size, hydrophilic polyvinylidene fluoride (PVDF), 25 mm Durapore® Membrane Millipore) and, once all components had reached room temperature, combined with the autoclaved base medium. Each of the experiments was performed in triplicate, with the exception of *Aspergillus Dimorphicus* and *Cordyceps Farinosa*, which were grown as replicates of 5.

3.2.3 Preparation of Cultures

For each strain, the Czapek-Dox broth was poured into pre-combusted GL45 bottles according to the table below, and sterilized by autoclaving at 121°C for 15 minutes. For the first two cultures, *Aspergillus dimorphicus* and *Cordyceps farinosa*, we used 20 bottles at 1L volume, but later switched to twelve 2L bottles instead, to prevent oxygen deprivation later in the growth phase. Butyl septa were sterilized by boiling them in 1M sodium hydroxide (NaOH) for one hour, washing them six times with MQ, and finally UV sterilising them. Once all components of the base medium were combined, 1 mL of the conidia suspension was inoculated into each bottle, and the bottles sealed with the butyl septa and GL45 hole caps.

Table 3: Composition of media with different isotopic labels

δ^2H of water	**Natural**	**100‰**	**200‰**	**400‰**
Non-labelled $NaHCO_3$ (µL of 90 g L^{-1} stock)	50	50	50	50
D_2O addition (µL of 9.9% stock)	0	11	19	34.5
^{13}C-HCO_3 addition (µL of 3 g L^{-1} stock)	0	150	150	150
Volume of all solutions (µL)	50	211	219	234.5
Volume of Growth medium (mL)	49.95	49.89	49.88	49.87
Final Volume of medium (mL)	50	50	50	50

3.2.4 Fungal Growth

The cultures were incubated at 25°C in the dark, and the head-space sampled periodically to determine the growth rate of the fungi, with the exception of the first culture. This was done by extracting 2mL of air from the head-space of each bottle with a syringe, and transferring it into 12mL Exetainers that were pre-flushed with helium for 10 minutes at a flow rate of

100mL/min. The CO_2 concentration of the samples was then determined via gas chromatography on a Hewlett Packard HP 5890 Series II Gas Chromatograph with a Thermal Conductivity Detector (TCD). For this, 1mL of gas was injected with an oven temperature of 70°C and a detector temperature of 130°C with helium as a carrier gas. The column used was a 30m HP-PLOT/Q (diameter 0.530mm, film thickness 40.0µm). The fungi were harvested when around 30% of the substrate had been respired into CO_2. However, *Phanerodontia chrysosporium* and *Yarrowia lipolytica* failed to grow according to CO_2 data and were therefore excluded from further analyses.

3.2.4.1 Growth

The growth process of the fungi was monitored via CO_2 measurements, which were converted to % substrate respired according to the following calculations:

$$\frac{ppm \times \text{headspace(L)}}{10^6} \times \frac{\text{dilution factor}}{\text{molar volume}} = C_{respired}(mol)$$

Head-space is the volume of the bottles – the volume of the medium

Dilution factor is 2mL sampled head-space in 12mL Exetainer = 6

Molar volume is taken as 22.4L/mol

$$\frac{C_{respired}(mol)}{C_{original}(mol)} \times 100\,\% = consumed\ substrate\,(\%)$$

$C_{respired}$ is the amount of carbon respired in mol of CO_2

$C_{original}$ is the amount of carbon originally added to the bottle in mol

3.2.4.2 Carbon Use Efficiency

Carbon use efficiency was calculated based on CO_2 data and weight of dry biomass, according to the calculation below. The conversion factor of 0.4338 biomass %C used to calculate gC of the biomass is an average of the values reported by Zhang and Elser[23]

$$Biomass\,(g) * Conversion\ factor = gC\,(biomass)$$

$$\frac{gC\,(biomass)}{(gC\,(biomass) + gC\,(CO\,2))} = Carbon\ use\ efficiency$$

3.2.5 Harvesting

When roughly 30% respiration of the substrate into CO_2 was observed, the growth medium was separated from the mycelial biomass by filtering it through a sterile miracloth and the media samples were collected in sterile Falcon tubes. Following a final pH determination of the samples, they were frozen at -20°C until further analysis. The biomass on the miracloth was washed three times with MQ, weighed to determine wet mass, then freeze dried. Finally, the dry weight was determined and the biomass stored at -20°C for use in a parallel project.

3.3 Sample Processing

3.3.1 Filtration

In order to remove any remaining biomass from the fungal culture media (exudate), the samples were then filtered via vacuum filtration through pre-combusted Glass Fibre GF/F (0.7µm) filters, or, when there was too much biomass, first through a GF/A (1.6µm) filter and then through GF/F.

3.3.2 Extraction

Before extraction, exudate samples were thawed at 4°C over night and 1 mL of the samples was removed and stored for measurement of antioxidant activity. The remainder of the medium was then used for liquid-liquid extraction of fungal metabolites. The solvent used was a 4:6 dichloromethane (DCM) to ethyl acetate (EtOAc) mixture, of which 4x 40mL were used for the extraction. The combined organic phase was then washed with 3x 40mL MQ, and the solvent subsequently evaporated at 40°C under argon. The dried extract was transferred out of the flasks by rinsing them with 3x 1.3mL of 4:6 DCM:EtOAc into combusted 4mL glass vials using a glass Pasteur pipette. The solvent was then evaporated at room temperature under argon, and the Total Medium Extracts (TME) were stored at -18°C.

3.4 UV-visible Spectroscopy Analyses

Prior to the GC-MS analysis of the extracted and derivatized TME, we probed the quality, as well as quantity of the compounds exuded into the medium via UV-Vis spectroscopy using a Specord 50 Plus spectrophotometer by Analytic Jena.

3.4.1 ABTS Antioxidant Assay

The antioxidant activity of the exudate samples (pre-extraction) was measured via a modified version of the radical cation decolourization assay after Re et al.[24] For the assay,

(2,2'-azino-bis (3-ethylbenzothiazoline-6-sulphonate ammonium)) (ABTS) was combined with potassium peroxodisulphate ($K_2S_2O_8$) and left to react overnight in the dark. The resulting solution was diluted with sodium acetate buffer (adjusted to pH 4.4 ± 0.1) the next day to form the working solution, with a distinct blue-green colour due to the ABTS•+ radical cation formation according to the reactions below.

$$ABTS + S_2O_8^{2-} \rightarrow ABTS^{\bullet+} + SO_4^{\bullet-} + SO_4^{2-}$$

$$ABTS + SO_4^{\bullet-} \rightarrow ABTS^{\bullet+} + SO_4^{2-}$$

Table 4: Reagents and dilutions for ABTS working solution

	Reagent	**Amount**	**MQ (mL)**
Buffer stock solutions	Sodium acetate trihydrate	1.3608g	50
	Glacial acetic acid	0.578mL	50
Buffer	Sodium acetate stock	22mL	
	Acetic acid stock	28mL	
			50
$K_2S_2O_8$ stock solution	Potassium peroxodisulphate	0.085g	5
ABTS stock solution	ABTS	0.02g	9.8
	Potassium peroxodisulphate stock	200µL	
ABTS working solution	ABTS stock	5mL	
	Buffer	95mL	

A trolox dilution series in methanol (MeOH) was prepared to serve as a standard curve, according to the table below. From each dilution point, 75µL was diluted in 3mL of the ABTS working solution, in triplicate, and the UV-Vis absorbance was measured at 731nm, (50nm/s and 0.02s integration time). Methanol was used as reference for time t0, while the measurements were done at time t30 to allow for complete reaction. A calibration curve of the absorbance decrease vs. trolox molar units was then plotted.

Table 5: Trolox concentrations for standard curve

Trolox µL of 1g/L stock	0	10	25	50	100	200	300	400	500	600
MeOH µL	1000	990	975	950	900	800	700	600	500	400
Trolox concentration in mM	0	0.04	0.10	0.20	0.40	0.80	1.20	1.60	2.00	2.40

Only the points from 0-0.2mM were used for the final curve as the media absorbance values never exceeded these

After a reference measurement was performed using MQ, 75µL of the fungal medium sample were diluted in 3mL of the ABTS working solution, in triplicate, and the UV-Vis absorbance was measured at 731nm as described above for trolox. The cuvettes were washed 3 times with MQ from a wash bottle between samples. The antioxidant activity of the sample media was then determined as Trolox Equivalent Antioxidant Capacity (TEAC), in nmol trolox g^{-1} dry fungal biomass according to the following equations:

$$\Delta A = [\frac{(A_{t0} - A_{t30})}{A_{t0}}] \times 100\,\%$$

ΔA is the absorbance decrease of the solution from 0 to 30 minutes in percent

A_{t0} is the absorbance of the solution at 0 minutes in cm^{-1}

A_{t30} is the absorbance of the solution at 30 minutes in cm^{-1}

$$n_{TROLOX} = \frac{(\Delta A - intercept)}{slope}$$

n_{TROLOX} is the amount of trolox with the equivalent absorbance decrease according to the calibration curve in µmol

ΔA is the absorbance decrease of the trolox solution from 0 to 30 minutes in cm^{-1}

intercept is the y-intercept of the calibration curve in cm^{-1}

slope is the slope of the calibration curve in cm^{-1}/µmol

From this molar trolox equivalent, the trolox equivalent of a blank medium without added bicarbonate was subtracted, before normalising the samples via their biomass according to the calculation below.

$$TEAC = \frac{n_{TROLOX}}{biomass}$$

TEAC is the Trolox Equivalent Antioxidant Capacity of the samples in nmol/g

n_{TROLOX} is the amount of TROLOX with the equivalent absorbance decrease according to the calibration curve in nmol

biomass is the weight of the dry fungal biomass in gram

3.4.2 Total Medium Extract Absorbance

In order to get a rough approximation of the concentration of the extracted samples, we dissolved 100% the TME in 3mL of acetonitrile (ACN) and measured the absorbance. This was done using a 4mL quartz cuvette, and measuring in the range of 200-800nm (50 nm/s and 0.02s integration time). A reference measurement was performed using ACN. Depending on the absorbance of the sample, it was then further diluted with ACN until the maximum

absorbance was between 0.1 and 1 cm^{-1}. Between each sample, the cuvette was washed 3 times with ACN using a glass Pasteur pipette.

3.5 Isotope Ratio Mass Spectrometry

3.5.1 Preparation for Elemental Analysis

In order to analyse the isotopic composition of the TME, the samples were dissolved in 5:1 DCM:MeOH and 25% TME transferred into pre-weighed silver (Sercon, smooth wall 9×3.5mm) and tin (IVA, smooth wall 9×3.5mm) capsules. After evaporating the samples under argon, they were stored in a desiccator over night and weighed the following day.

3.5.2 Compound Specific Isotope Analysis

The derivatized samples will be analysed on a GC-IRMS for Compound-Specific Isotopic Analysis (CSIA).

3.6 Derivatization of TME for GC analyses

3.6.1 Acetylation

10% of the TME were derivatized via acetylation of OH-bearing compounds. This was done by adding 100µL acetic anhydride and 20µL of 1-methyl imidazole to the dried samples, and then heating them at 80°C for 20 minutes. After the vials cooled down, the reaction was stopped via the addition of 0.5mL of MQ and a liquid-liquid extraction with 4x 0.5mL DCM was performed. The pooled organic phase was then dried under argon, while heating the vials at 45°C to ensure any water evaporates completely. Finally, the dried samples were resuspended in 50µL of EtOAc, vortexed, sonicated and the supernatant collected for analysis.

3.6.2 Trimethylsilylation

50% of the TME was derivatized via trimethylsilylation (TMS) of OH- bearing compounds, forming ether derivates. The reagent used was 50µL of N,O-bistrifluoroacetamide (BSTFA), as well as 100µL of pyridine as a catalyst and solvent. After addition of the reagents, the samples were heated at 70°C for one hour to ensure reaction completion. Once the samples cooled down, care was taken to evaporate the reagents completely by drying the samples under argon, redissolving them in 100µL isopropanol when almost dry, and drying them again, twice. Finally, the dried samples were resuspended in 200µL EtOAc right before

injecting them into the GC-MS instrument. As some TMS derivatives are known to degrade within hours[25], the samples were only derivatized on the day of measurement and then kept in the autosampler vial rack until injection (~19°C).

3.7 Gas Chromatography-Mass Spectrometry Analysis

GC-MS measurement of 1µL of the samples via splitless injection was done on a single quadrupole ISQ QD (Thermo Scientific, Bremen, Germany), using Electron Impact ionization with the injection temperature set to 310°C, transfer line to 280°C, ion source to 230°C, and a helium carrier gas flow rate of 1.4mL/min. The FID (flame ionization detector; Thermo Scientific, Bremen, Germany) was set to 300°C with air 350 mL/min, H_2 at 35 mL/min and makeup at 40 mL/min. A SLB-IL60 (30 m x 0.25 mm I.D., 0.20 µm, Merck KGaA, Darmstadt, Germany) column was connected via a 3 port Multi-Channel Device (MCD) (Trajan Scientific) to acquire MS and FID data simultaneously. A temperature program was set as: 5 min at 60°C, then a 10°C/min increase to 150°C, then a 4°C/min increase to 280°C with a 20 min hold, and finally a 4°C/min increase to 300°C with a 5 min hold. The whole program had a run time of 76.5 min and a scanning range of 45-700 amu.

3.8 Gas Chromatography-Mass Spectrometry Data Analysis

3.8.1 Acetylated TME

The FID spectra of the acetylated samples were compared to that of a blank using the Qual browser of the Xcalibur software by Thermo Scientific. Due to the high noise level and lack of peaks in the Total Ion Current (TIC) spectra, the samples were additionally viewed in ion map mode. Unfortunately, no acetylated compounds were readily identifiable as molecular or fragment ions.

3.8.2 Trimethylsilylated TME

The TIC spectra of 3 samples of each species were grouped along with the spectra of three blanks, using the Qual browser of the Xcalibur software by Thermo Scientific. Potential peaks were manually selected by comparing the samples to the blanks, and to each other. Only peaks that do not occur in the blanks, but do occur in at least 2 of the replicates, were exported via the Add Peaks function and transferred to a spreadsheet via the Export Clipboard Peaklist option. A noise reduction was performed in the MS spectrum of the peaks by subtracting ranges before and after the peak to be analysed, and the remaining mass list exported to the NIST library browser for preliminary analysis. Additionally, a list of quinones potentially present in the TME was created, the structures drawn via ChemDraw, and a table created from the masses of the predicted fragments (Appendix). Finally, a Layout was created for each Quinone based on mass ranges of the headgoup fragment and two fragments expected from a break after the first double bond. The sample spectra were then manually searched with the Layout and results recorded in a spreadsheet.

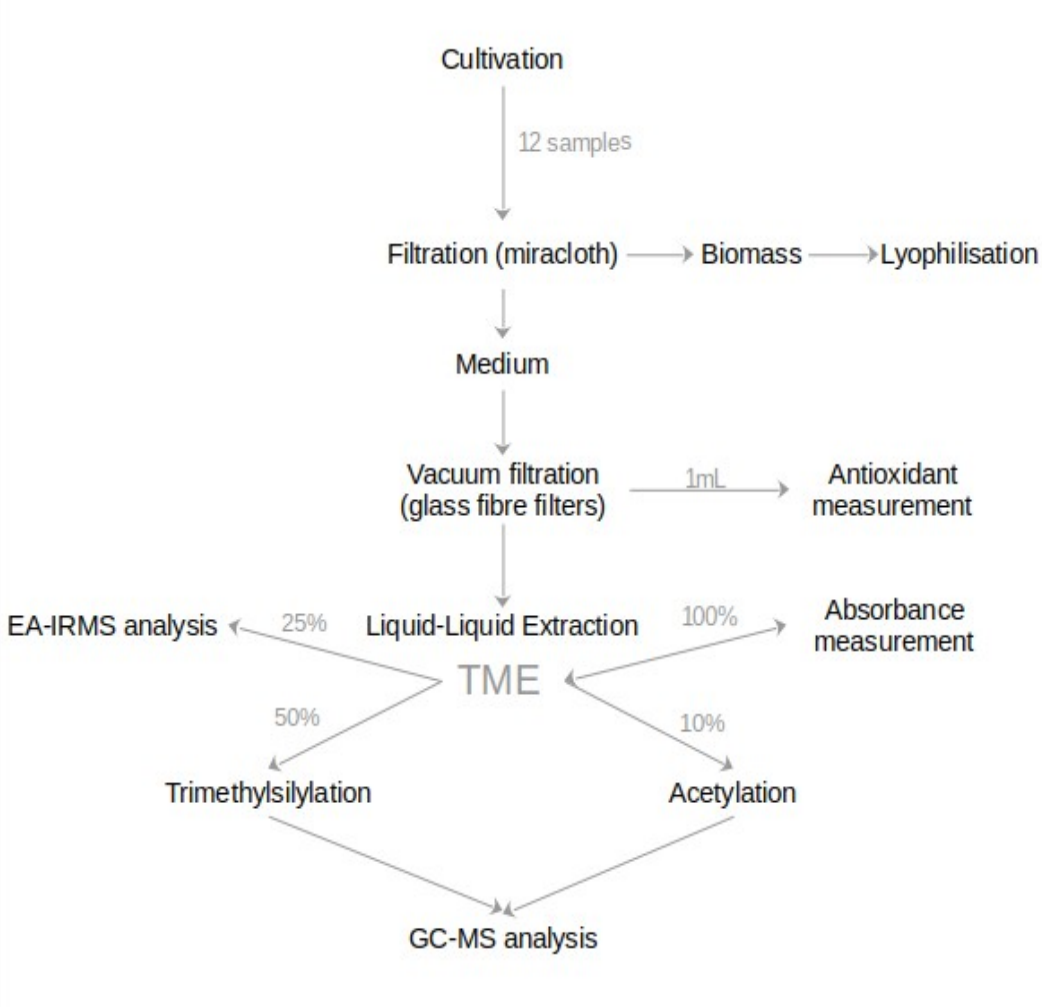

Figure 2: Workflow schematic of fungal media extraction and analysis

4 Results

4.1 Culturing

4.1.1 Growth

Both the rate as well as the amount of CO_2 produced for the total period of incubation varied widely between the species. *Cordyceps farinosa* had an exponential CO_2 production rate and the highest amount of CO_2 when harvested. The remaining species' production rates were more similar, exhibiting approximately linear growth. Excepted from this are the species *Yarrowia lipolytica* and *Phanerodontia chrysosporium*, which failed to grow based on both CO_2 data as well as visible biomass production, and were thus excluded from further analysis.

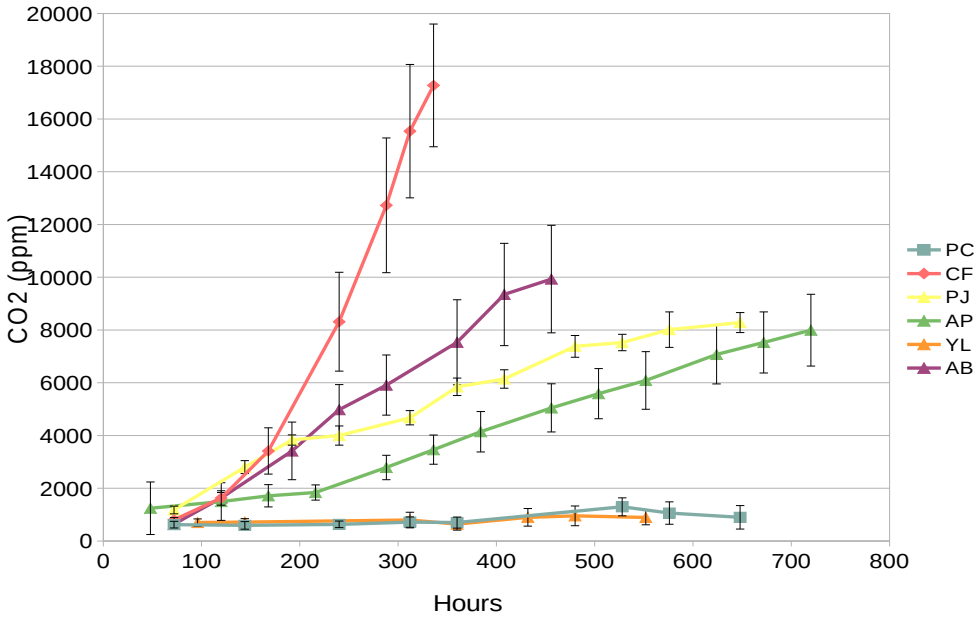

Figure 3: Comparison of mean CO_2 production (ppm) ± SD production by species. For each data point n=12 except for CF where n=20. Note: Aspergillus Dimorphicus was harvested after 14 days (no CO_2 data available)

The average weight of the dry fungal biomass was approximately 0.1g for each sample, except for *Acremonium polychromum* which weighed slightly less at 0.07g. The final pH of the media ranged from 3.43 to 6.80 (initial pH was approximately 7.3) and appears to have no significant correlation to biomass production ($R^2 = 0.427$).

Table 6: Mean weight (g) ± SD of dry fungal biomass and pH of growth media after harvesting (n=12 except for AD and CF where n=20)

Species	Weight (g)	pH
AD	0.10±0.02	3.83±0.11
CF	0.11±0.01	4.50±0.24
PJ	0.11±0.01	6.12±0.09
AB	0.09±0.01	3.43±0.36
AP	0.07±0.01	6.80±0.06

4.1.2 Carbon Use Efficiency

The approximate carbon use efficiency (CUE) of the individual species ranged between 33-51%.

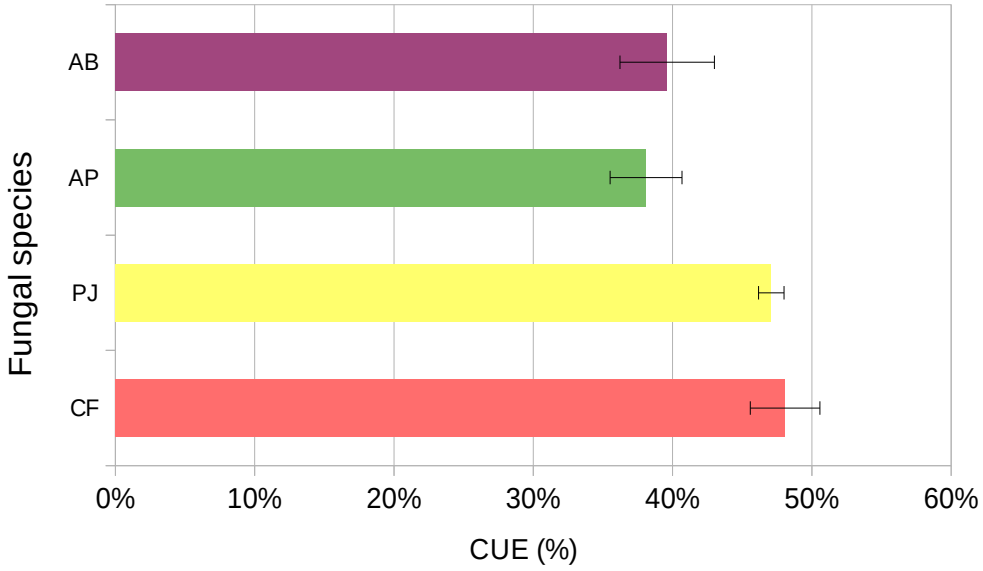

Figure 4: Comparison of mean carbon use efficiency (CUE) ± SD (n.=12) in glucose medium

4.2 Antioxidant Assay

The average radical scavenging activity (TEAC) of the fungal growth media after biomass harvest and vacuum filtration is 125 nmol g^{-1} of biomass, with *Penicillium janczewskii* having by far the lowest values at 60 ± 5. The graph below shows the values per species after the subtraction of the blank medium control TEAC values. It should be noted that the reference curve used for the calculations was reduced to the first 4 points in order to limit the values to the range in which the samples absorbed.

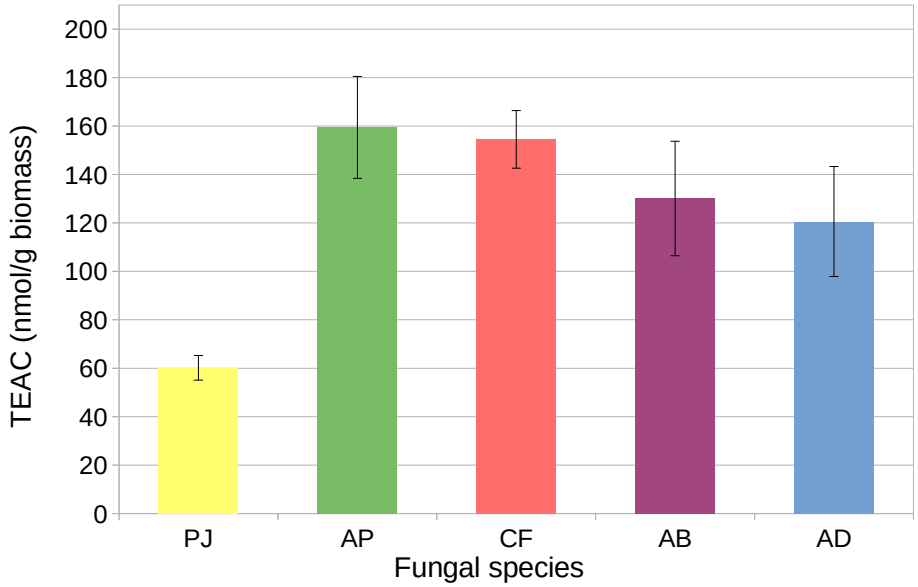

Figure 5: Comparison of mean TEAC values ± SD (n=4)

4.3 Total Medium Extract Absorbance

The local absorbance maxima of the TME in acetonitrile generally lay at about 275nm. However, the exact values varied between 250 and 280nm depending on the species, with *Aspergillus dimorphicus* absorbing at a lower wavelength than the rest. The absorbance varied greatly between the species, with *Aspergillus dimorphicus* and *Aspergillus brasiliensis* absorbing outside of the 0.1-1cm^{-1} range and thus being diluted to 50% and 25%, respectively. It must also be noted that the overall maxima could not be used as there was a lot of noise in the <220nm region.

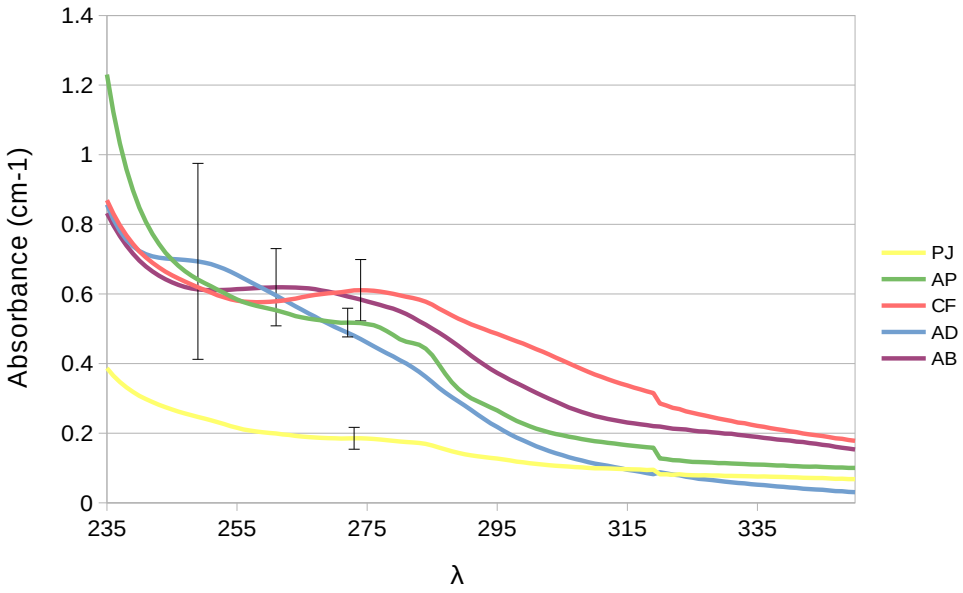

Figure 6: Comparison of mean local maxima of UV absorption ± SD (n=3) of fungal TME by species. Note: AD was diluted to 50% and AB to 25% TME, while for the rest 100% TME was used.

4.4 Isotope Ratio Mass Spectrometry

Due to the fact that the IRMS was inoperative during the analysis period of this thesis, no results on the isotopic composition of the samples were obtained.

4.5 Gas Chromatography-Mass Spectrometry analysis

4.5.1 Acetylated TME

The GC-MS analysis of the acetylated TME samples yielded spectra with many peaks on the FID that do not appear in the spectra of extraction blanks (no medium added) (Fig.6). However, most of these were not distinguishable on the MS, which had a high background noise level ranging from about 3-9x10^6 (Fig.7). The two peaks that are clearly recognisable on MS were determined to be 1-methyl imidazole and dehydroacetic acid, as denoted by the NIST library browser with a 96.1% probability; these are contaminants of the derivatisation reagents. Furthermore, when viewed in the Ion Map mode strong bleeding from the reagent contaminants is visible.

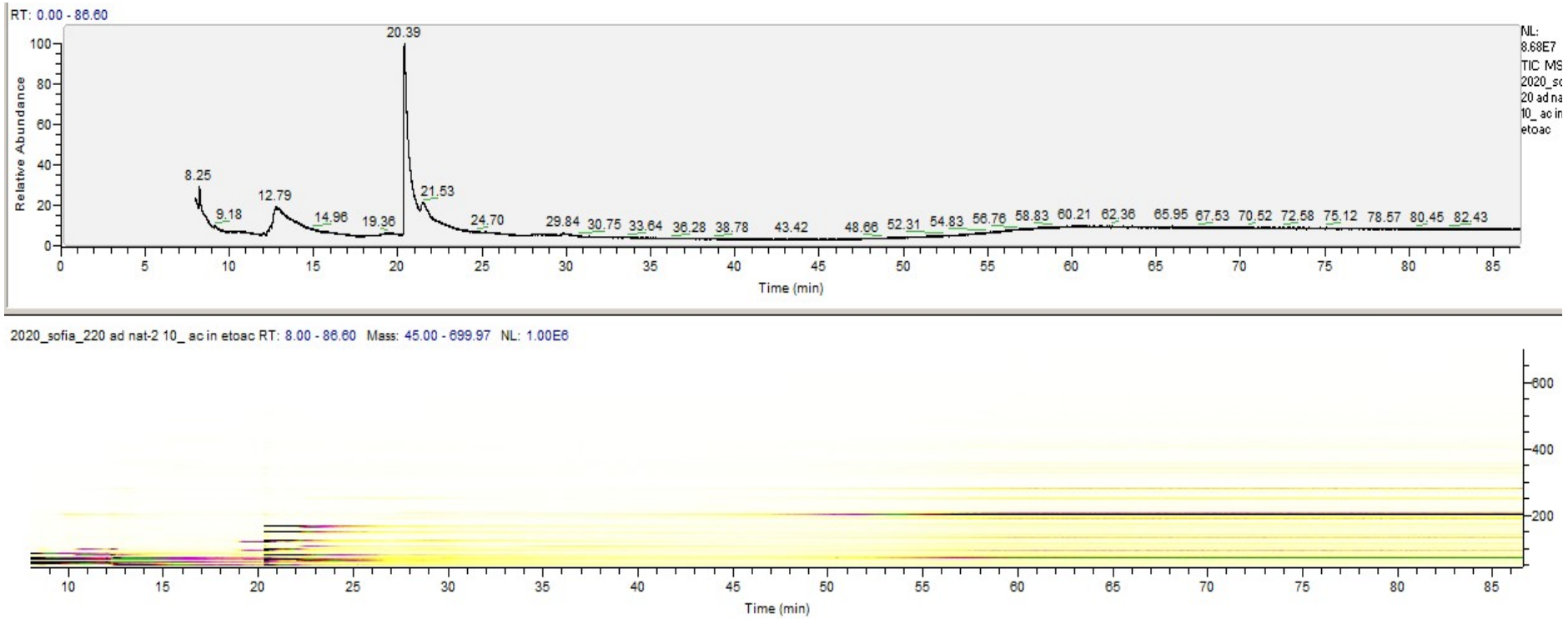

Figure 7: visualisation of noise level of acetylated sample as MS spectrum (top) and ion map (bottom; normalized to 1e6)

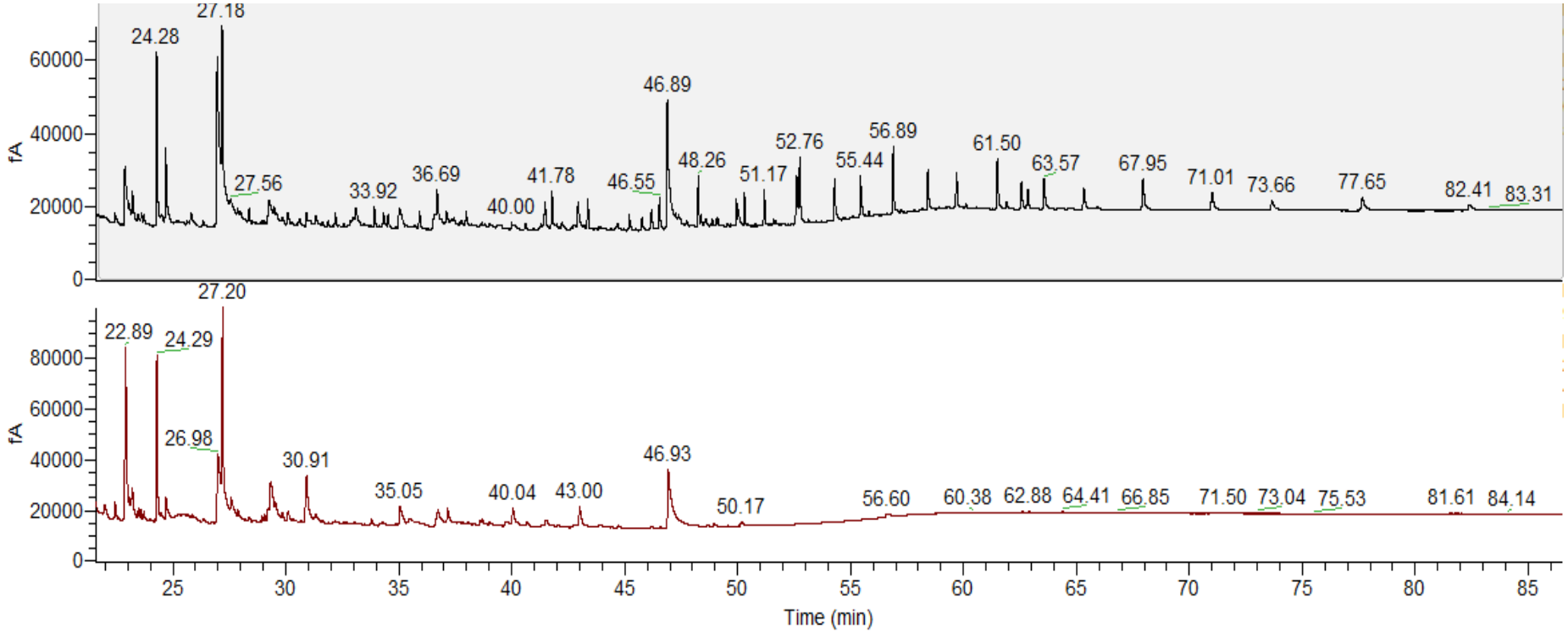

Figure 8: Comparison between FID spectra of acetylated sample (top) versus method blank (bottom; normalised to ion intensity of 10^6)

4.5.2 Trimethylsilylated TME

For the TMS-derivatized samples, the peaks detected via FID are also visible in the MS spectra. However, most of the peaks in the spectra can also be found in the method blanks. After elimination of those peaks, the remaining peaks were taken into consideration for identification and grouped by species, with *Aspergillus brasiliensis* containing by far the most peaks.

The compounds identified were either matched with library spectra from the NIST mass spectra library in the Xcalibur software, or with specific fragments stemming from a list of quinones that was compiled (Appendix). The minimum requirement for identification via the NIST library was 25% and above match between spectra. Quinone identification was achieved by finding the headgroup of the quinone plus other ions resulting from fragmentation of the isoprenoid chain, in accordance with published GC-MS spectra or as predicted by simulated fragmentation using ChemDraw.

Table 7:Compounds found in fungal TMEs via NIST library and hypothesised fragmentation spectra of selected quinones Dimethylmenaquinone (DMMK) and Ubiquinone (UQ)

	Apex RT	NIST ID	NIST %	Q fragments found
AB	**15.3**			
	17.81	Triethylamine	76.40%	
	22.11	4-Isopropylcyclohexanone	57.10%	
	26.46			
	40.34	Ricinoleic acid	29.40%	
	48.5			
AP	**32.65**	3,4-Dimethyl-o-phenylenediamine	34.30%	
	34.87			**DMMK 10-0/1/2**
	36.23	γ Dodecalactone	34.50%	
PJ	**15.34**			
	21.68	Phenol, 2,4-bis(1,1-dimethylethyl)-	98%	
	23.68	n-Hexylmethylamine	61%	
	25.07			
	28.87			
CF	**31.85**			**UQ-10-0**

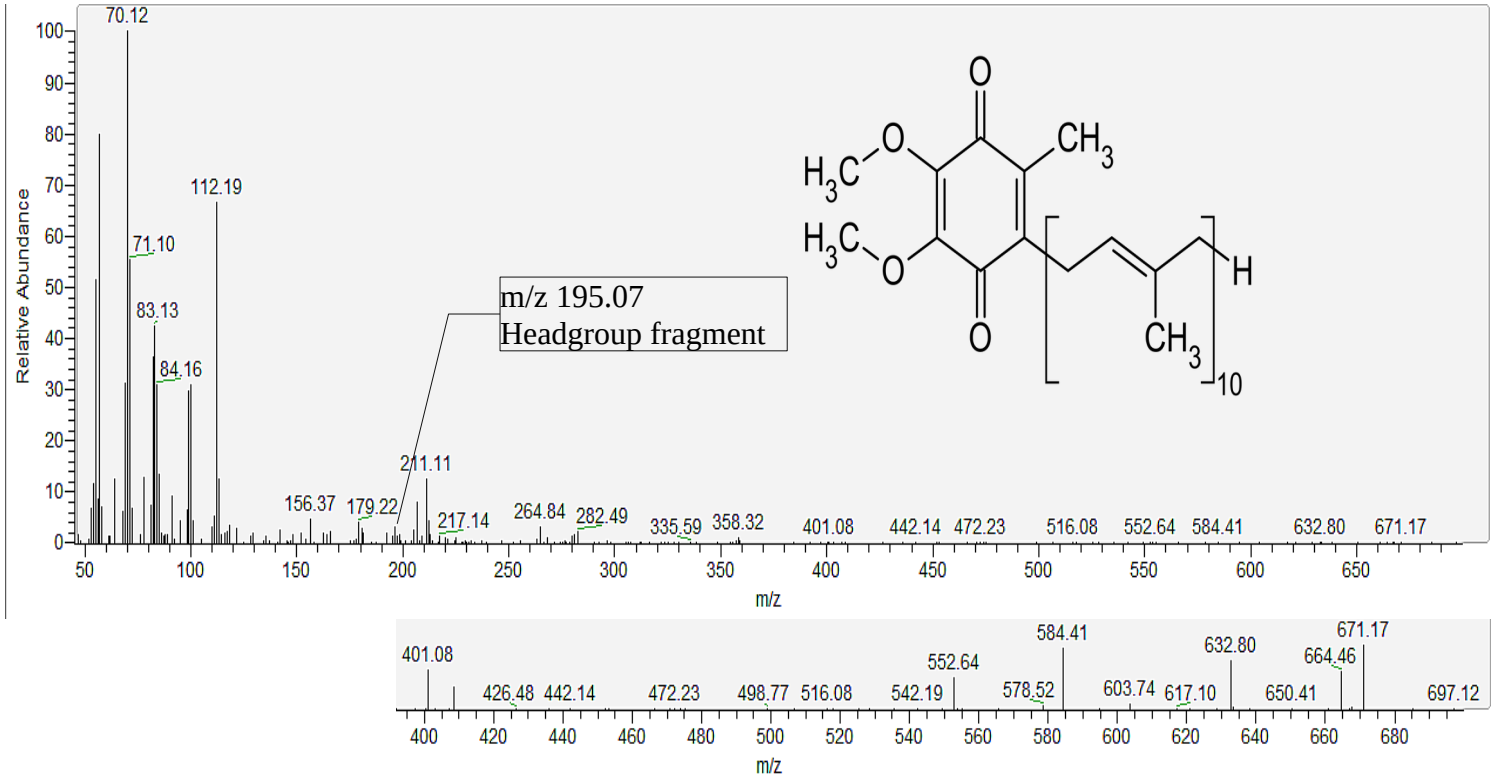

Figure 9: MS spectrum of Cordyceps farinosa, RT 31.85, containing ions predicted for the fragmentation of Ubiquinone; Lower image is the amplified masses at the end of the scanning range

5 Discussion

5.1 Culturing

5.1.1 Growth

The variation in CO_2 production rates of the fungi seem to have no link to the taxonomic classification of the fungi within Ascomycota, with the Ascomycetes growing at varying rates. However, the two strains that did not grow were the Basidiomycete and the Saccharomycete. Basidiomycetes are known to grow more slowly under laboratory conditions and further optimisation of the cultivation protocol is required (J. Jansa, personal communication, Biomed CAS, 2021).

5.1.2 Carbon Use Efficiency

The CUE of 33-52% is relatively high compared to the means calculated by Sinsabaugh et al from a variety of terrestrial soil and litter studies[26]. Since, per definition, CUE is inversely proportional to carbon-based exudate, this would indicate that the fungal growth medium contains few compounds of biological origin. However, it must be noted that the values in the study mentioned were from field studies of soil respiration and hence had varying conditions as well as microbial compositions, and generally increased at higher fungal:bacterial populations. Other reviews of CUE values show a large variation in values, ranging from 30-83% based on changes in environmental and stoichiometric variables[27].

5.2 Antioxidant Assay

The TEAC values obtained for the ABTS free radical scavenging assay show that while the majority of species are in the same range of antioxidant activity, *Penicillium janczewskii*'s activity is over 50% lower. The activities do not seem to correspond to any other measurements, including CO_2 production and pH.

It must be noted, however, that the calculated values range between 60 and 160 nmol trolox g^{-1} of dried fungal biomass, which is 1-2 orders of magnitude lower than similar experiments in the literature[2829], though in those experiments it is an extract of dried biomass, not a growth medium, being analysed.

Furthermore, since all measured sample absorbances are at the low end of the original calibration curve, only the first 4 values of the curve were used for calculations. This low

number of reference values decreases the precision of calculations. Additionally, the initial absorbance of the ABTS solution used in this assay is significantly higher than the ~0.7 cm^{-1} found in the literature[243031], meaning that low levels of antioxidant activity may be harder to quantify.

5.3 Total Medium Extract Absorbance

Using EtOAc, we often experienced high and erratic peaks in the UV range leading to unusable spectra. Due to this fact we chose Acetonitrile as the final solvent to measure the absorbance spectra as it absorbs at a low wavelength (λ_{end} 190nm[32]) and resulted in the cleanest spectra. Although there were still high noise levels in some samples, they were all <220nm and we could thus use the local maxima >230nm as a gauge for the quantity of material in the TME samples.

The two *Aspergilli* species had by far the greatest absorbance, even needing to be diluted to stay within the 0.1-1 cm^{-1} range. This also directly corresponds to the colour intensity of the TME, which was strongest for *Aspergillus brasiliensis* and second most intense for *Aspergillus dimorphicus*.

5.4 Isotope Ratio Mass Spectrometry

5.4.1 Elemental Analysis

The results from EA-IRMS will allow us to determine how much of the isotopically labelled water and inorganic carbon was used by the fungi for biosynthesis and then exuded into the medium.

5.4.2 Compound Specific Isotope Analysis

The compound specific isotope analysis via GC-IRMS will allow confirmation of biosynthesis of compounds via increased isotopic labelling. This will allow for the currently selected peaks to be either analysed in more detail, or be excluded from the results.

5.5 Derivatization

5.5.1 Acetylation

The mixing of 1-methyl imidazole and acetic anhydride resulted in the formation of a yellow substance that is only soluble in polar organic solvents. This occurred in all samples, standards, and method blanks and led to partial precipitation when we attempted to dissolve

the dried samples in EtOAc for analysis. The precipitate was likely an intermediate of the derivatization reagents; nevertheless, due to only the supernatant being used for analysis, we may unfortunately have lost some compounds in the precipitate.

5.5.2 Trimethylsilylation

Upon drying the reagents and attempting to resuspend them in EtOAc, *Aspergillus dimorphicus* precipitated and could not be resuspended in ethyl acetate, acetone, or ethanol. Therefore, it was excluded from GC-MS analysis. *Aspergillus brasiliensis* also formed a slight precipitate but the mixture was much lighter – closer to the colour before derivatization – and we were able to collect the supernatant for analysis due to the large particle size of the precipitate. A possible explanation for this is that the pyridine, which was stored in a vial in the fridge, contained moisture and this degraded the BSTFA and derivatives.

5.6 Gas Chromatography-Mass Spectrometry Data Analysis

5.6.1 Acetylation

Unfortunately, due to the lack of analyte peaks in the MS spectra, no qualitative interpretation can be done for the acetylated samples. The two peaks that do show up on MS were identified via NIST as reagent and reagent intermediate peaks. The Ion Map also shows significant bleeding from those signals, which would hide any sample peaks and would explain the high noise level.

FID, however, shows many promising peaks in the samples that do not show up in the blanks. This may mean that there are biosynthesised compounds present in the TME but were not able to be ionized in the ion source.

5.6.2 Trimethylsilylation

While there are many peaks detected in the trimethylsilylated samples, both via FID and MS, most of them can also be found in the blanks and must therefore be excluded from analysis. Many of those were tentatively identified via NIST and found to be either solvent peaks that are eluting after the solvent front, derivatization reagents that were not fully evaporated, or potential plastic contaminants. This could be due to corrosive solvents coming into extended contact with plastic components during sample preparation.

Nevertheless, there are also peaks found in the samples that look unique to the individual species and do not occur in the blanks. *Aspergillus brasiliensis* contained the highest number of peaks as well as the most intense colouration – which may point towards the detection of these coloured compounds via MS. Additionally, both *Cordyceps farinosa*, as well as *Acremonium polychromum* contained multiple ions from the predicted fragmentation of quinones, which are known antioxidants[3334]. These species also showed the highest antioxidant activity in the ABTS assay. However, the fragments usually appeared in all samples around retention time 30-40 minutes, at which time the method blanks also contained peaks, and are thus not enough to definitively label the peaks as coming from individual quinones.

5.7 Future work

Unfortunately, not being able to perform the isotopic analysis of the samples leaves a lot of uncertainties on the origin of compounds in the samples. IRMS will allow us to narrow down the potential exudate peaks and thereby focus our efforts of identifying compounds. Elemental Analysis of the samples will additionally shed light on the ratio of carbon and hydrogen incorporation from inorganic carbon sources and water, respectively.

Increasing the species diversity to include more Basidiomycota may allow for phylogenetically-linked correlations to become apparent, and adjusting the ABTS concentration in the antioxidant assay protocol to a lower initial absorbance would allow for more accurate comparison to values found in literature.

Regarding sample preparation, the derivatization techniques must be optimised to allow for GC-MS analysis. For the acetylation of TME, using a different catalyst and base than the 1-methyl imidazole may prevent the formation of the precipitate (M. Waser, personal communication, JKU, 2021) – though the ionizability of the sample compounds remains to be seen. Using the trimethylsilylation, a completely moisture free workflow is essential. It may also be beneficial to omit the final evaporation and re-dissolution steps and choose a column in which the reagents may be used as solvents to limit both the variety of solvents contained in the sample, as well as the amount of pipetting and, consequently, contact with plastic the samples have.

Furthermore, additional MS analysis using LC-MS to identify molecular ions can be used to complement the fragment spectra.

6 Conclusion

This research aimed to investigate a component of the below-ground carbon flux based on fungal metabolic activity. The focus was on the incorporation of carbon and exudation of biologically synthesised compounds.

From the gathered CO_2 data, as well as the TME absorbance measurements, the differences in carbon exudate quantities between fungal cultures could be inferred, showing clear variation between species. The quality of the exuded compounds, characterised by antioxidant activity as well as colour intensity, varied as well, and, while further research on the accuracy of the exact TEAC values is needed, a clear deviation from the mean value was seen for *Penicillium janczewskii*. GC-FID analysis of the acetylated samples additionally showed a high diversity of compounds, and, though the nature of these compounds require MS analysis, the findings are in line with existing research on the metabolomics of fungi functional guilds[12].

The effective separation of these compounds via GC was also accomplished, as demonstrated by the peak distribution via FID especially. This is essential for future IRMS analysis, which will greatly assist the identification and characterisation of these compounds[18].

Therefore, this project produced insights into the exudates and growth of axenic fungal cultures under regulated growth conditions, with equipment parameters and methodology being tested and optimised for this research.

7 References

1. Ussiri, D. A. N. & Lal, R. *Carbon Sequestration for Climate Change Mitigation and Adaptation*. (Springer International Publishing : Imprint: Springer, 2017). doi:10.1007/978-3-319-53845-7.
2. Lal, R. Carbon sequestration. *Philos. Trans. R. Soc. B Biol. Sci.* **363**, 815–830 (2008).
3. *Mycorrhizal mediation of soil: fertility, structure, and carbon storage*. (Elsevier, 2017).
4. Litton, C. M. & Giardina, C. P. Below-ground carbon flux and partitioning: global patterns and response to temperature. *Funct. Ecol.* **22**, 941–954 (2008).
5. Moore, D., Robson, G. D. & Trinci, A. P. J. *Twenty first century guidebook to fungi*. (Cambridge university press, 2020).
6. Dikec, J. *et al.* Hyphal network whole field imaging allows for accurate estimation of anastomosis rates and branching dynamics of the filamentous fungus Podospora anserina. *Sci. Rep.* **10**, 3131 (2020).
7. Boddy, L., Wood, J., Redman, E., Hynes, J. & Fricker, M. D. Fungal network responses to grazing. *Fungal Genet. Biol.* **47**, 522–530 (2010).
8. Klein, D. A. & Paschke, M. W. Filamentous Fungi: the Indeterminate Lifestyle and Microbial Ecology. *Microb. Ecol.* **47**, (2004).
9. Nehls, U., Grunze, N., Willmann, M., Reich, M. & Küster, H. Sugar for my honey: Carbohydrate partitioning in ectomycorrhizal symbiosis. *Phytochemistry* **68**, 82–91 (2007).
10. Lindahl, B. D. & Tunlid, A. Ectomycorrhizal fungi – potential organic matter decomposers, yet not saprotrophs. *New Phytol.* **205**, 1443–1447 (2015).
11. Shah, F. *et al.* Ectomycorrhizal fungi decompose soil organic matter using oxidative mechanisms adapted from saprotrophic ancestors. *New Phytol.* **209**, 1705–1719 (2016).
12. Taylor, D. L. *et al.* Structure and resilience of fungal communities in Alaskan boreal forest soilsThis article is one of a selection of papers from The Dynamics of Change in Alaska's Boreal Forests: Resilience and Vulnerability in Response to Climate Warming. *Can. J. For. Res.* **40**, 1288–1301 (2010).

13. Talbot, J. M., Martin, F., Kohler, A., Henrissat, B. & Peay, K. G. Functional guild classification predicts the enzymatic role of fungi in litter and soil biogeochemistry. *Soil Biol. Biochem.* **88**, 441–456 (2015).
14. Thrane, U., Anderson, B., Frisvad, J. C. & Smedsgaard, J. The exo-metabolome in filamentous fungi. in *Metabolomics* (eds. Nielsen, J. & Jewett, M. C.) vol. 18 235–252 (Springer Berlin Heidelberg, 2007).
15. Dunn, W. B. *et al.* Mass appeal: metabolite identification in mass spectrometry-focused untargeted metabolomics. *Metabolomics* **9**, 44–66 (2013).
16. Metabolomics: Current analytical platforms and methodologies. *TrAC Trends Anal. Chem.* **24**, 285–294 (2005).
17. Boccard, J., Veuthey, J.-L. & Rudaz, S. Knowledge discovery in metabolomics: An overview of MS data handling. *J. Sep. Sci.* **33**, 290–304 (2010).
18. Weber, R., Selander, E., Sommer, U. & Viant, M. A Stable-Isotope Mass Spectrometry-Based Metabolic Footprinting Approach to Analyze Exudates from Phytoplankton. *Mar. Drugs* **11**, 4158–4175 (2013).
19. Amelung, W., Brodowski, S., Sandhage-Hofmann, A. & Bol, R. Chapter 6 Combining Biomarker with Stable Isotope Analyses for Assessing the Transformation and Turnover of Soil Organic Matter. in *Advances in Agronomy* vol. 100 155–250 (Elsevier, 2008).
20. Czapek, F. Studies on the formation of nitrogen fixation and protein crops. *Beitr Chem Physiol U Pahtol* **1**, 540–560 (1902).
21. Dox, A. W. *The Intracellular Enzyms of Penicillium and Aspergillus, With Special Reference to Those of Penicillium Camemberti*. vol. 120 (U.S. Dept. of Agriculture, Bureau of Animal Industry, 1910).
22. Thom, C. & Raper, K. B. *A Manual of the Aspergilli*. (Williams & Wilkins, 1945).
23. Zhang, J. & Elser, J. J. Carbon:Nitrogen:Phosphorus Stoichiometry in Fungi: A Meta-Analysis. *Front. Microbiol.* **8**, 1281 (2017).
24. Re, R. *et al.* Antioxidant activity applying an improved ABTS radical cation decolorization assay. *Free Radic. Biol. Med.* **26**, 1231–1237 (1999).

25. Quéro, A. *et al.* Improved stability of TMS derivatives for the robust quantification of plant polar metabolites by gas chromatography–mass spectrometry. *J. Chromatogr. B* **970**, 36–43 (2014).
26. Sinsabaugh, R. L. *et al.* Stoichiometry of microbial carbon use efficiency in soils. *Ecol. Monogr.* **86**, 172–189 (2016).
27. Manzoni, S., Taylor, P., Richter, A., Porporato, A. & Ågren, G. I. Environmental and stoichiometric controls on microbial carbon-use efficiency in soils. *New Phytol.* **196**, 79–91 (2012).
28. Kirakosyan, A., Seymour, E. M., Llanes, D. E. U., Kaufman, P. B. & Bolling, S. F. Chemical profile and antioxidant capacities of tart cherry products. *Food Chem.* **115**, 20–25 (2009).
29. Kirakosyan, A. *et al.* Antioxidant Capacity of Polyphenolic Extracts from Leaves of *Crataegus laevigata* and *Crataegus monogyna* (Hawthorn) Subjected to Drought and Cold Stress. *J. Agric. Food Chem.* **51**, 3973–3976 (2003).
30. Olszowy, M. & Dawidowicz, A. L. Is it possible to use the DPPH and ABTS methods for reliable estimation of antioxidant power of colored compounds? *Chem. Pap.* **72**, 393–400 (2018).
31. Nenadis, N., Wang, L.-F., Tsimidou, M. & Zhang, H.-Y. Estimation of Scavenging Activity of Phenolic Compounds Using the ABTS $^{\bullet+}$ Assay. *J. Agric. Food Chem.* **52**, 4669–4674 (2004).
32. Pretsch, E., Bühlmann, P. & Affolter, C. *Structure determination of organic compounds: tables of spectral data*. (Springer, 2000).
33. Kruk, J., Szymańska, R., Nowicka, B. & Dłużewska, J. Function of isoprenoid quinones and chromanols during oxidative stress in plants. *New Biotechnol.* **33**, 636–643 (2016).
34. Belozerskaya, T. A. & Gessler, N. N. Reactive oxygen species and the strategy of antioxidant defense in fungi: A review. *Appl. Biochem. Microbiol.* **43**, 506–515 (2007).

8 Appendix

8.1 List of possible quinone fragments

	Code name	Molecular Formula	Headgroup	Fragments expected from break right after the 1st double bond	Other fragments from literature
ubiquinones	**UQ-10:0**	C59H110N0O4S0	195.06	237.11, 645.72	70.07, 71.07, 57.05
	UQ-10:1	C59H108N0O4S0	195.06	235.09, 645.72	68.07, 69.07, 55.05
	UQ-10:2	C59H106N0O4S0	195.06	235.09, 643.71	68.07, 69.07, 55.05
	UQ-10:3	C59H104N0O4S0	195.06	235.09, 641.69	68.07, 69.07, 55.05
	UQ-10:4	C59H102N0O4S0	195.06	235.09, 639.68	68.07, 69.07, 55.05
	UQ-10:5	C59H100N0O4S0	195.06	235.09, 637.66	68.07, 69.07, 55.05
	UQ-10:6	C59H98N0O4S0	195.06	235.09, 635.64	68.07, 69.07, 55.05
	UQ-10:7	C59H96N0O4S0	195.06	235.09, 633.63	68.07, 69.07, 55.05
	UQ-10:8	C59H94N0O4S0	195.06	235.09, 631.61	68.07, 69.07, 55.05
	UQ-10:9	C59H92N0O4S0	195.06	235.09, 629.60	68.07, 69.07, 55.05
	UQ-10:10 (coQ 10)	C59H90N0O4S0	195.06	235.09, 627.58	68.07, 69.07, 55.05
	UQ-9:0	C54H100N0O4S0	195.06	237.11, 575.64	70.07, 71.07, 57.05
	UQ-9:1	C54H98N0O4S0	195.06	235.09, 575.64	68.07, 69.07, 55.05
	UQ-9:2	C54H96N0O4S0	195.06	235.09, 573.63	68.07, 69.07, 55.05
	UQ-9:3	C54H94N0O4S0	195.06	235.09, 571.61	68.07, 69.07, 55.05
	UQ-9:4	C54H92N0O4S0	195.06	235.09, 569.60	68.07, 69.07, 55.05
	UQ-9:5	C54H90N0O4S0	195.06	235.09, 567.58	68.07, 69.07, 55.05
	UQ-9:6	C54H88N0O4S0	195.06	235.09, 565.57	68.07, 69.07, 55.05
	UQ-9:7	C54H86N0O4S0	195.06	235.09, 563.55	68.07, 69.07, 55.05
	UQ-9:8	C54H84N0O4S0	195.06	235.09, 561.54	68.07, 69.07, 55.05
	UQ-9:9	C54H82N0O4S0	195.06	235.09, 559.52	68.07, 69.07, 55.05
caldariellaquinones	**CQ10:0**	C59H106N0O2S2	222.99	265.03, 645.72	70.07, 71.07, 57.05
	CQ10:1	C59H104N0O2S2	222.99	263.02, 645.72	68.07, 69.07, 55.05
	CQ10:2	C59H102N0O2S2	222.99	263.02, 643.71	68.07, 69.07, 55.05
	CQ10:3	C59H100N0O2S2	222.99	263.02, 641.69	68.07, 69.07, 55.05
	CQ10:4	C59H98N0O2S2	222.99	263.02, 639.68	68.07, 69.07, 55.05
	CQ10:5	C59H96N0O2S2	222.99	263.02, 637.66	68.07, 69.07, 55.05
	CQ10:6	C59H94N0O2S2	222.99	263.02, 635.64	68.07, 69.07, 55.05
	CQ10:7	C59H92N0O2S2	222.99	263.02, 633.63	68.07, 69.07, 55.05
	CQ10:8	C59H90N0O2S2	222.99	263.02, 631.61	68.07, 69.07, 55.05
	CQ10:9	C59H88N0O2S2	222.99	263.02, 629.60	68.07, 69.07, 55.05
	CQ10:10	C59H86N0O2S2	222.99	263.02, 627.58	68.07, 69.07, 55.05

	Code name	Molecular Formula	Headgroup	Fragments expected from break right after the 1st double bond	Other fragments from literature
sulfolobusquinones	**SQ10:0**	C59H106N0O2S1	191.02	233.06, 645.72	70.07, 71.07, 57.05
	SQ10:1	C59H104N0O2S1	191.02	231.04, 645.72	68.07, 69.07, 55.05
	SQ10:2	C59H102N0O2S1	191.02	231.04, 643.71	68.07, 69.07, 55.05
	SQ10:3	C59H100N0O2S1	191.02	231.04, 641.69	68.07, 69.07, 55.05
	SQ10:4	C59H98N0O2S1	191.02	231.04, 639.68	68.07, 69.07, 55.05
	SQ10:5	C59H96N0O2S1	191.02	231.04, 637.66	68.07, 69.07, 55.05
	SQ10:6	C59H94N0O2S1	191.02	231.04, 635.64	68.07, 69.07, 55.05
	SQ10:7	C59H92N0O2S1	191.02	231.04, 633.63	68.07, 69.07, 55.05
	SQ10:8	C59H90N0O2S1	191.02	231.04, 631.61	68.07, 69.07, 55.05
	SQ10:9	C59H88N0O2S1	191.02	231.04, 629.60	68.07, 69.07, 55.05
	SQ10:10	C59H86N0O2S1	191.02	231.04, 627.58	68.07, 69.07, 55.05
	SQ-9:0	C54H96N0O2S1	191.02	233.06, 575.64	70.07, 71.07, 57.05
	SQ-9:1	C54H94N0O2S1	191.02	231.04, 575.64	68.07, 69.07, 55.05
	SQ-9:2	C54H92N0O2S1	191.02	231.04, 573.63	68.07, 69.07, 55.05
	SQ-9:3	C54H90N0O2S1	191.02	231.04, 571.61	68.07, 69.07, 55.05
	SQ-9:4	C54H88N0O2S1	191.02	231.04, 569.60	68.07, 69.07, 55.05
	SQ-9:5	C54H86N0O2S1	191.02	231.04, 567.58	68.07, 69.07, 55.05
	SQ-9:6	C54H84N0O2S1	191.02	231.04, 565.57	68.07, 69.07, 55.05
	SQ-9:7	C54H82N0O2S1	191.02	231.04, 563.55	68.07, 69.07, 55.05
	SQ-9:8	C54H80N0O2S1	191.02	231.04, 561.54	68.07, 69.07, 55.05
	SQ-9:9	C54H78N0O2S1	191.02	231.04, 559.52	68.07, 69.07, 55.05
plastoquinones	**PQ-10:0**	C58H108N0O2S0	149.06	191.10, 645.72	70.07, 71.07, 57.05
	PQ-10:1	C58H106N0O2S0	149.06	189.09, 645.72	68.07, 69.07, 55.05
	PQ-10:2	C58H104N0O2S0	149.06	189.09, 643.71	68.07, 69.07, 55.05
	PQ-10:3	C58H102N0O2S0	149.06	189.09, 641.69	68.07, 69.07, 55.05
	PQ-10:4	C58H100N0O2S0	149.06	189.09, 639.68	68.07, 69.07, 55.05
	PQ-10:5	C58H98N0O2S0	149.06	189.09, 637.66	68.07, 69.07, 55.05
	PQ-10:6	C58H96N0O2S0	149.06	189.09, 635.64	68.07, 69.07, 55.05
	PQ-10:7	C58H94N0O2S0	149.06	189.09, 633.63	68.07, 69.07, 55.05
	PQ-10:8	C58H92N0O2S0	149.06	189.09, 631.61	68.07, 69.07, 55.05
	PQ-10:9	C58H90N0O2S0	149.06	189.09, 629.60	68.07, 69.07, 55.05
	PQ-10:10	C58H88N0O2S0	149.06	189.09, 627.58	68.07, 69.07, 55.05

	Code name	Molecular Formula	Headgroup	Fragments expected from break right after the 1st double bond	Other fragments from literature
menaquinones	**MK-10:0**	C61H108N0O2S0	185.06	227.27, 645.72	70.07, 71.07, 57.05
	MK-10:1	C61H106N0O2S0	185.06	225.09, 645.72	68.07, 69.07, 55.05
	MK-10:2	C61H104N0O2S0	185.06	225.09, 643.71	68.07, 69.07, 55.05
	MK-10:3	C61H102N0O2S0	185.06	225.09, 641.69	68.07, 69.07, 55.05
	MK-10:4	C61H100N0O2S0	185.06	225.09, 639.68	68.07, 69.07, 55.05
	MK-10:5	C61H98N0O2S0	185.06	225.09, 637.66	68.07, 69.07, 55.05
	MK-10:6	C61H96N0O2S0	185.06	225.09, 635.64	68.07, 69.07, 55.05
	MK-10:7	C61H94N0O2S0	185.06	225.09, 633.63	68.07, 69.07, 55.05
	MK-10:8	C61H92N0O2S0	185.06	225.09, 631.61	68.07, 69.07, 55.05
	MK-10:9	C61H90N0O2S0	185.06	225.09, 629.60	68.07, 69.07, 55.05
	MK-10:10	C61H88N0O2S0	185.06	225.09, 627.58	68.07, 69.07, 55.05
methionaquinones	**MTK-10:0**	C61H108N0O2S1	217.03	259.07, 645.72	70.07, 71.07, 57.05, 203.01, 701.79
	MTK-10:1	C61H106N0O2S1	217.03	257.06, 645.72	68.07, 69.07, 55.05, 203.01, 701.79
	MTK-10:2	C61H104N0O2S1	217.03	257.06, 643.71	68.07, 69.07, 55.05, 203.01, 701.79
	MTK-10:3	C61H102N0O2S1	217.03	257.06, 641.69	68.07, 69.07, 55.05, 203.01, 701.79
	MTK-10:4	C61H100N0O2S1	217.03	257.06, 639.68	68.07, 69.07, 55.05, 203.01, 701.79
	MTK-10:5	C61H98N0O2S1	217.03	257.06, 637.66	68.07, 69.07, 55.05, 203.01, 701.79
	MTK-10:6	C61H96N0O2S1	217.03	257.06, 635.64	68.07, 69.07, 55.05, 203.01, 701.79
	MTK-10:7	C61H94N0O2S1	217.03	257.06, 633.63	68.07, 69.07, 55.05, 203.01, 701.79
	MTK-10:8	C61H92N0O2S1	217.03	257.06, 631.61	68.07, 69.07, 55.05, 203.01, 701.79
	MTK-10:9	C61H90N0O2S1	217.03	257.06, 629.60	68.07, 69.07, 55.05, 203.01, 701.79
	MTK-10:10	C61H88N0O2S1	217.03	257.06, 627.58	68.07, 69.07, 55.05, 203.01, 701.79

	Code name	Molecular Formula	Headgroup	Fragments expected from break right after the 1st double bond	Other fragments from literature
demethylmenaquinones	**DMK-10:0**	C60H106N0O2S0	171.04	213.09, 645.72	70.07, 71.07, 57.05
	DMK-10:1	C60H104N0O2S0	171.04	211.07, 645.72	68.07, 69.07, 55.05
	DMK-10:2	C60H102N0O2S0	171.04	211.07, 643.71	68.07, 69.07, 55.05
	DMK-10:3	C60H100N0O2S0	171.04	211.07, 641.69	68.07, 69.07, 55.05
	DMK-10:4	C60H98N0O2S0	171.04	211.07, 639.68	68.07, 69.07, 55.05
	DMK-10:5	C60H96N0O2S0	171.04	211.07, 637.66	68.07, 69.07, 55.05
	DMK-10:6	C60H94N0O2S0	171.04	211.07, 635.64	68.07, 69.07, 55.05
	DMK-10:7	C60H92N0O2S0	171.04	211.07, 633.63	68.07, 69.07, 55.05
	DMK-10:8	C60H90N0O2S0	171.04	211.07, 631.61	68.07, 69.07, 55.05
	DMK-10:9	C60H88N0O2S0	171.04	211.07, 629.60	68.07, 69.07, 55.05
	DMK-10:10	C60H86N0O2S0	171.04	211.07, 627.58	68.07, 69.07, 55.05
demethylmenaquinones	**DMK-10:0**	C60H106N0O2S0	171.04	213.09, 645.72	70.07, 71.07, 57.05
	DMK-10:1	C60H104N0O2S0	171.04	211.07, 645.72	68.07, 69.07, 55.05
	DMK-10:2	C60H102N0O2S0	171.04	211.07, 643.71	68.07, 69.07, 55.05
	DMK-10:3	C60H100N0O2S0	171.04	211.07, 641.69	68.07, 69.07, 55.05
	DMK-10:4	C60H98N0O2S0	171.04	211.07, 639.68	68.07, 69.07, 55.05
	DMK-10:5	C60H96N0O2S0	171.04	211.07, 637.66	68.07, 69.07, 55.05
	DMK-10:6	C60H94N0O2S0	171.04	211.07, 635.64	68.07, 69.07, 55.05
	DMK-10:7	C60H92N0O2S0	171.04	211.07, 633.63	68.07, 69.07, 55.05
	DMK-10:8	C60H90N0O2S0	171.04	211.07, 631.61	68.07, 69.07, 55.05
	DMK-10:9	C60H88N0O2S0	171.04	211.07, 629.60	68.07, 69.07, 55.05
	DMK-10:10	C60H86N0O2S0	171.04	211.07, 627.58	68.07, 69.07, 55.05